Optimization design and experiment of the variable differential gear train planting mechanism

Xiong Zhao[1], Ziwei Liu[1], Yuanwu Jia[2], Xingxiao Ma[1], Pengfei Zhang[3], Jianneng Chen[1*]

(1. *School of Mechanical Engineering, Zhejiang Sci-Tech University, Hangzhou 310018, China*;
2. *Xi'an International University Engineering College, Xi'an 710077, China*;
3. *Hangzhou Vocational & Technical College, Hangzhou 310018, China*)

Abstract: In order to improve the adaptability of the planting mechanism for different plant spacings, a variable differential gear train planting mechanism based on precise pose and trajectory control was proposed by combining the open chain 2R rod group and the variable differential gear train. According to the pose requirements of receiving seedling point, transporting seedling point and planting point, three precise pose points of constrained planting trajectory were determined. Through the three-position motion generation structural synthesis method, combined with computer-aided optimization design software, a set of mechanism parameters that meet the planting requirements were optimized. Based on the optimized mechanism parameters, by only changing the coordinates of two trajectory shape control points, three planting trajectories with key point position information adapted to 300 mm, 400 mm and 500 mm plant spacing were obtained by interpolation, and three pairs of total transmission ratio of three groups of variable differential gear trains were calculated. When distributing the total transmission ratio of the mechanism, the fixed axis gear train and the differential gear train are combined. The fixed axis gear train included a pair of non-circular gear pairs and a pair of positive gear pairs, which were convenient for disassembly and assembly. The former drives the sun gear at variable speed, and the latter drives the planet carrier at uniform speed. Based on this structure, the transmission ratio of the positive gear pair is –1, and the transmission ratio of the differential gear train is 0.5. The sub-transmission ratio of the single-stage non-circular gear pair was calculated and the pitch curves of three pairs of non-circular gears were solved. Three pairs of non-circular gear pairs with different transmission ratios were replaced in turn and three sets of planting mechanisms were modeled in three dimensions. The virtual prototype motion simulation was completed by ADAMS software, and the physical prototype was built for vegetable pot seedling planting test. The theoretical solution was consistent with the attitude and trajectory of the actual test. When the test sample size was 100 plants, the actual average plant spacing was measured to be 303 mm, 402 mm, and 503 mm, with errors of 1.3%, 1.25%, and 1.88%. The width of the moving hole was 72 mm, 70 mm, and 71 mm, and the planting success rate were 94%, 96%, and 95%. The test results verified the correctness of the optimization design results of the mechanism, indicating that the variable differential gear train planting mechanism can adapt to a variety of plant spacing and has good planting effect.

Keywords: plant spacing, planting mechanism, variable differential gear train, precise pose, trajectory control, parameter optimization

1 Introduction

There are many kinds of crops with mechanized transplanting demand in China[1-3], and their requirements for plant spacing are not the same. Even the same crop has different requirements for plant spacing in different seasons and regions. The planting mechanism is the core working part of the transplanter. The plant spacing and other agronomic requirements of the crop determine the complexity and diversity of the planting mechanism. Its performance will directly affect the seedling rate, seedling injury rate and planting quality after transplanting[4,5]. At present, the existing semi-automatic or full-automatic transplanting machines are equipped with a wide variety of planting mechanisms, such as clamp type, chain clamp type, seedling guide tube type, flexible disc type and duckbill type[6-10], but they can only meet the plant spacing requirements of one crop, and there are relatively few mechanisms with adjustable plant spacing. The multiple semi-automatic dry-field pot seedling transplanter developed by Ferrari company in Italy was a seedling-guiding tube structure. The seedlings were put into the feeding tube manually when working. When the feeding nozzle at the end of the feeding tube rotates to the feeding inlet of the seedling-guiding tube, the feeding nozzle opens. The seedlings fall into the seedling ditch by gravity, covering the soil and pressing, and completing the planting process. The mechanism has stable transmission, reliable structure, high efficiency and is not easy to hurt seedlings. Although the plant spacing can be adjusted by controlling the forward speed of the unit. but when the plant

Biographies: Xiong Zhao, PhD, Professor, research interest: mechanism design, non-circular gear transmissions, and agricultural machinery, Email: zhaoxiong@zstu.edu.cn; **Ziwei Liu**, MS candidate, research interest: agricultural machinery, Email: 1153565139@qq.com; **Yuanwu Jia**, MS, research interest: mechanical design and control, Email: 717280124@qq.com; **Xingxiao Ma**, MS, research interest: agricultural machinery, Email: 2416771239@qq.com; **Pengfei Zhang**, Lecturer, research interest: agricultural machinery, Email: 527677162@qq.com.
*Corresponding author: Jianneng Chen, PhD, Professor, research interest: machine design, non-circular gear transmissions and control, and agricultural machinery. Faculty of Mechanical Engineering and Automation, Zhejiang Sci-Tech University, Hangzhou 310018, China. Tel: +86-13065701536, Email: jiannengchen@zstu.edu.cn.

spacing increases, the seedlings that fall into the seedling ditch by gravity are gradually affected by inertia. This way will seriously affect the location, uprightness and transplanting quality of seedlings, and is prone to lodging. Therefore, the planting mechanism can only maintain a fixed plant spacing[11]. The HD144 type automatic transplanting machine developed by Australian Transplant Systems company, when working, 4-6 seedlings were taken out from the tray by the sliding needle type seedling picking manipulator, and then the pot seedlings were transferred to the conveying cup, and the pot seedling conveying cup was used for secondary seedling throwing. The machine has a high degree of automation, fast operation speed and adjustable plant spacing. However, its plant spacing adjustment depends on the change and debugging of the PLC control system of the whole machine. It is difficult to operate and has high cost. It does not meet the agronomic requirements of China and has not been widely introduced and promoted[12,13]. Nippon Liguan Corporation in Japan has developed a PVHR2 transplanting machine[14], which was equipped with a seven-bar planting mechanism with two degrees of freedom to achieve a specific trajectory and attitude of the planting nozzle. It is easy to control and suitable for small plot operations. It has the function of planting deep profiling and strong terrain adaptability. The duckbill planter can realize transplanting on the film, and the planting qualification rate is high. Although the plant spacing can be adjusted by controlling the forward speed of the unit, due to the fixed planting trajectory, the plant spacing will be reduced. Li et al.[15] focused on the PVHR2 transplanting machine, optimized and processed the rods of the original planting mechanism to achieve a 150mm plant spacing required for dense planting of peppers. They replaced the rods on both sides of the original planting mechanism, altered the planting trajectory, reduced the hole width, and obtained satisfactory experimental results. However, the disassembly and assembly of the rods were somewhat cumbersome, and the adjustment of the plant spacing was inefficient. Zhao et al.[16] and Chen et al.[17,18] proposed a non-circular gear planetary wheel system planting mechanism, with the sun gear fixed to the frame. The sun wheel was fixed to the frame, and the planting mouth was driven by the non-circular gear transmission to move according to the set trajectory[19,20]. Duckbill shaped planter it achieved seedling picking, seedling transportation and planting operations by cooperating with the cam opening and closing duckbill shaped planter. It is a high-efficiency mechanism scheme with stable transmission and reliable structure. However, in order to ensure a better planting effect, it is necessary to realize the "zero-speed" planting at the lowest point of planting, that is, the trajectory

of the planter is stationary relative to the ground at the planting moment, forming a "ring buckle" of appropriate size, which requires that the speed of the planting mechanism must match the speed of the transplanter. It is difficult to adjust the plant spacing. If the basic parameters of the mechanism (rod length, gear center distance, etc.) and the position of the planting key points were kept unchanged, the target planting efficiency was given, the moving speed of the transplanting machine was matched, and the control point was used to adjust the shape of the planting trajectory so that the ring formed by the moving trajectory can be adjusted within the appropriate numerical range.

In order to improve the adaptability of planting mechanism to different plant spacing, this paper proposes a variable differential gear train planting mechanism based on precise pose and trajectory control. On the basis of meeting the pose requirements of the seedling point, the seedling point and the planting point, the mechanism parameters are optimized based on the three-position motion generation mechanism synthesis method; the coordinates of two trajectory shape control points are changed, multiple planting trajectories adapted to different plant spacings through interpolation fitting are obtained, and the total transmission ratio of the variable differential gear train are calculate; The total transmission ratio distribution scheme is designed to solve the pitch curve of many pairs of non-circular gears. Several pairs of non-circular gear pairs with different transmission ratios were replaced in turn, and three-dimensional modeling, motion simulation and physical prototype test of the planting mechanism were carried out to verify the correctness of the optimization design results of the mechanism and its adaptability to different plant spacing.

2   Working principle of the mechanism

As shown in Figure 1, the main components of the mechanism are gearbox, positive gear pair, non-circular gear pair, differential gear train and duckbill shaped planter. The theoretical model of the mechanism can be expressed as a combination of an 2R open chain rod group and a variable differential gear train: the planet carrier (crank) is recorded as a rod L_1, and its rotation center (center point) is A_0; the straight-line segment (connecting rod) connecting the center of the planetary gear with the tip of the duckbill shaped planter is recorded as the rod L_2, and its rotation center (dot) is A_c. During the planting operation, the variable differential gear train planting mechanism has two power transmission routes. The first power transmission route is: the active positive gear rotates at a constant speed under the drive of the power input shaft, and the driven positive gear is meshed with it and fixedly connected with
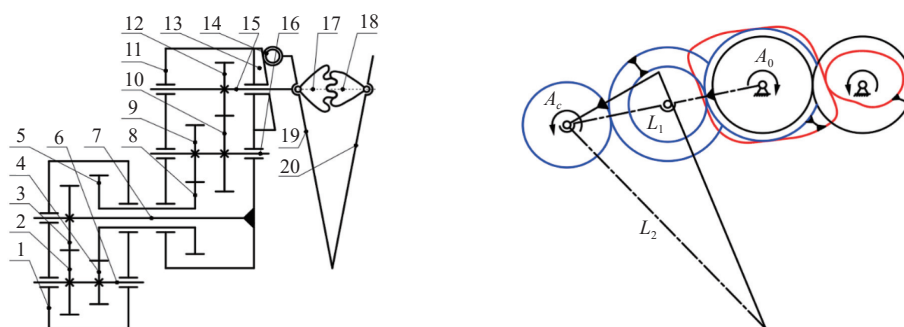
1. Gear box 2. Active spur gear 3. Driven spur gear 4. Active non-circular gear 5. Driven non-circular gear 6. Power input shaft 7. Driven gear shaft 8. Sun gear 9. Firstly idler gear 10. Secondly idler gear 11. Planet carrier 12. Planetary gear 13. Cam 14. Roller 15. Planetary gear shaft 16. Idler gear shaft 17. Left rotary gear seat 18. Right rotary gear seat 19. Left seedling duckbill 20. Right seedling duckbill

Figure 1   Variable differential gear train planting mechanism structure diagram

the planet carrier to drive the planet carrier to rotate at a constant speed; the second power transmission route is: the active non-circular gear rotates at a uniform speed under the drive of the power input shaft, and the driven non-circular gear engages with it and is fixed to the sun gear in the differential gear train. The two-stage non-uniform transmission is realized by meshing the sun gear, the intermediate gear and the planetary gear. Under the combined action of a uniformly rotating planetary frame and a variable-speed rotating solar wheel, the planetary shaft fixed to the planetary wheel makes a periodic non-uniform swing in the opposite direction to the planetary frame, thereby achieving complex trajectory and attitude requirements. The left and right rotating gear seats are hinged with the planetary shaft to form a revolute pair. The left and right shaped planters are respectively fixed to the left and right rotating gear seats, and the cam is fixed on the planetary shaft and fixed to the planet carrier. When the planetary shaft drives the duckbill shaped planter to rotate, the roller fixed with the left duckbill shaped planter drives the left and right rotating gear seats to open and close the duckbill shaped planter under the collision of the cam.

3   Design method of variable differential gear train mechanism

3.1   Analysis of the transmission ratio

As shown in Figure 2, the variable differential gear train is composed of a fixed-axis gear train and a differential gear train. The fixed-axis gear train includes a pair of non-circular gear pairs and a pair of positive gear pairs that are convenient for disassembly and assembly. The non-circular gear pair drives the sun gear at variable speeds, and its transmission ratio changes with the change of the planting trajectory. The positive gear pair drives the planet carrier at a constant speed, and its transmission ratio remains unchanged. The variable differential gear train mechanism is analyzed. Assuming that ω_i ($i=1,2,\ldots,9$) is the angular velocity (rad/s) of each component in the transmission system, the differential gear train transmission can be calculated as Equation (1)

$$m = i_{59}^8 = \frac{\omega_5 - \omega_8}{\omega_9 - \omega_8} \tag{1}$$

Active positive gear 1 and active non-circular gear 3 are fixed, $\omega_1 = \omega_3$; the driven gear 2 is fixedly connected with the planet carrier 8, $\omega_2 = \omega_8$; the driven non-circular gear 4 is fixed with the sun gear 5, $\omega_4 = \omega_5$; the transmission ratio of the positive gear pair is i_{12}, non-circular gear transmission as shown in Equation (2).

$$i_{34} = \frac{\omega_3}{\omega_4} = \frac{\omega_1}{m\omega_9 + (1-m)\left(\dfrac{\omega_1}{i_{12}}\right)} \tag{2}$$

The first and last gears rotate in the same direction, and the transmission ratio is positive. Considering the non-uniform swing of the planetary shaft relative to the planetary carrier in the opposite direction during the actual operation of the mechanism, $i_{12}=-1$; considering that the shape of the pitch curve of the first-stage gear transmission of the non-circular gear pair does not meet the processing conditions, $m=0.5$, Equation (3) is obtained.

$$i_{34} = \frac{2\omega_1}{\omega_9 - \omega_1} = \frac{-2\omega_8}{\omega_9 + \omega_8} = \frac{-2\dfrac{\mathrm{d}\phi_1}{\mathrm{d}t}}{\dfrac{\mathrm{d}\phi_2}{\mathrm{d}t} + \dfrac{\mathrm{d}\phi_1}{\mathrm{d}t}} \tag{3}$$

According to Equation (3), the transmission ratio of non-circular gear pair can be obtained by solving the rotation angle (ϕ_1 and ϕ_2) relationship between rod L_1 and rod L_2 in the 2R open chain rod group.
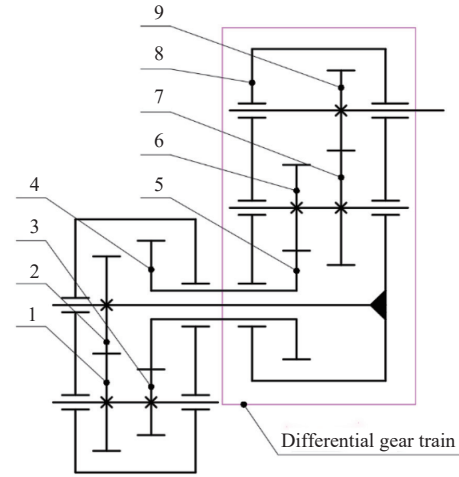
1. Active spur gear 2. Driven spur gear 3. Active non-circular gear 4. Driven non-circular gear 5. Sun gear 6. Firstly idler gear 7. Secondly idler gear 8. Planet carrier 9. Planetary gear

Figure 2   Principle diagram of variable differential gear train transmission system

3.2   Synthesis of three-position motion generation structural

In this paper, the connecting rods in the 2R open chain rod group are required to pass through several given positions in sequence according to a certain orientation. In the rigid body guidance of the linkage mechanism, the position of the linkage plane can be determined by the azimuth of any point on the linkage plane and any selected line[21-26]. As shown in Figure 3, when the plane is at the i-th position, the P point on it is $P_i(x_i, y_i)$ and the azimuth of $P_i S_i$ is θ_i, i=1, 2, 3. When the end of the connecting rod moves from $P_1(x_1, y_1)$ to $P_i(x_i, y_i)$, the dot moves from $A_{c1}(x_{c1}, y_{c1})$ to $A_{ci}(x_{ci}, y_{ci})$. The coordinate transformation of the two is shown in Equation (4).

$$\begin{bmatrix} A_{ci}^{\mathrm{T}} \\ 1 \end{bmatrix} = [D_{1i}] \begin{bmatrix} A_{c1}^{\mathrm{T}} \\ 1 \end{bmatrix} \tag{4}$$

where, D_{1i} is the general displacement matrix of rigid body:

$$[D_{1i}] = \begin{bmatrix} D_{11i} & D_{12i} & D_{13i} \\ D_{21i} & D_{22i} & D_{23i} \\ D_{31i} & D_{32i} & D_{33i} \end{bmatrix} \tag{5}$$

where,

$D_{11i} = \cos\theta_{1i}$, $D_{12i} = -\sin\theta_{1i}$, $D_{13i} = x_i - x_i\cos\theta_{1i} + y_i\sin\theta_{1i}$

$D_{21i} = \sin\theta_{1i}$, $D_{22i} = \cos\theta_{1i}$, $D_{23i} = y_i - x_i\sin\theta_{1i} - y_i\cos\theta_{1i}$

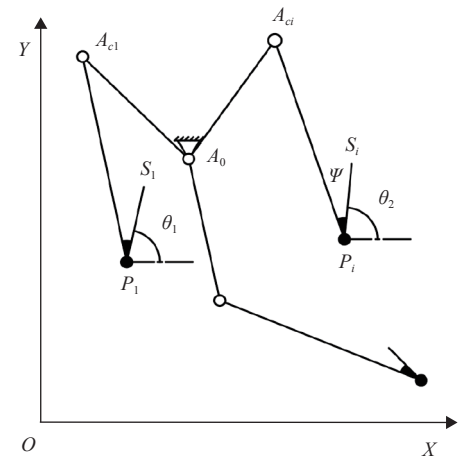$D_{31i} = 0$, $D_{32i} = 0$, $D_{33i} = 1$

Figure 3   Plane motion diagram of rigid body

$\theta_{1i} = \theta_i - \theta_1$ is the rotation angle of the i-th position of the connecting rod plane relative to the first position. According to the constant condition of rod length, there is a constraint equation:

$$[A_{ci} - A_0]^{\mathrm{T}}[A_{ci} - A_0] = [A_{c1} - A_0]^{\mathrm{T}}[A_{c1} - A_0] \qquad (6)$$

Substitute Equation (6) into Equation (4), and arrange it:

$$\begin{aligned} A_{i1}(x_0 x_{c1} + y_0 y_{c1}) + A_{i2}(y_0 x_{c1} - x_0 y_{c1}) + A_{i3}x_0 + \\ A_{i4}y_0 + A_{i5}x_{c1} + A_{i6}y_{c1} + A_{i7} = 0 \end{aligned} \qquad (7)$$

where,

$$A_{i1} = 1 - D_{11i}, \ A_{i2} = D_{12i}, \ A_{i3} = -D_{13i}, A_{i4} = -D_{23i}$$
$$A_{i5} = D_{11i}D_{13i} + D_{21i}D_{23i}, \ A_{i6} = D_{12i}D_{13i} + D_{22i}D_{23i}$$
$$A_{i7} = \frac{D_{13i}^2 + D_{23i}^2}{2}$$

For the three-position problem, any point in the connecting rod plane can be used as the hinge point. Or any point in the fixed plane can be used as a fixed hinge point (center point). This paper gives the exact pose points P_1 (seedling point), P_2 (seedling point) and P_3 (planting point), whose corresponding azimuth angles are θ_1, θ_2, θ_3 respectively. When the center point A_0 is (x_0, y_0), then Equation (7) can be transferred to a two-dimensional linear equation system about the point $A_{c1}(x_{c1}, y_{c1})$.

$$\begin{cases} G_{20}x_{c1} + K_{20}y_{c1} + N_{20} \\ G_{30}x_{c1} + K_{30}y_{c1} + N_{30} \end{cases} \qquad (8)$$

where,

$$G_{20} = A_{21}x_0 + A_{22}y_0 + A_{25}, \ K_{20} = A_{21}y_0 - A_{22}x_0 + A_{26}$$
$$N_{20} = A_{23}x_0 - A_{24}y_0 + A_{27}, \ G_{30} = A_{31}x_0 + A_{32}y_0 + A_{35}$$
$$K_{30} = A_{31}y_0 - A_{32}x_0 + A_{36}, \ N_{30} = A_{33}x_0 + A_{34}y_0 + A_{37}$$

The expression of the point coordinate can be obtained by solving Equation (8)

$$\begin{cases} x_{c1} = \dfrac{N_{20}K_{30} - N_{30}K_{20}}{G_{30}K_{20} - G_{20}K_{30}} \\ y_{c1} = \dfrac{N_{20}G_{30} - N_{30}G_{20}}{G_{20}K_{30} - G_{30}K_{20}} \end{cases} \qquad (9)$$

In order to establish the mechanism scale solution domain, the length of the crank is constrained. Given the length of the crank $A_0 A_{c1}$ is r, there is:

$$(x_{c1} - x_0)^2 + (y_{c1} - y_0)^2 = r^2 \qquad (10)$$

Substituting Equation (10) into Equation (9), the distribution curve of the center point $A_0(x_0, y_0)$ can be obtained.

$$\begin{aligned} [N_{20}K_{30} - N_{30}K_{20} - x_0(G_{30}K_{20} - G_{20}K_{30})]^2 + [N_{20}G_{30} - N_{30}G_{20} - \\ y_0(G_{20}K_{30} - G_{30}K_{20})]^2 = r^2(G_{20}K_{30} - G_{30}K_{20})^2 \end{aligned} \qquad (11)$$

By applying the numerical algorithm, let x_0 take values continuously in a given solution interval with a certain step length, and obtain the circle point and center point curve (Burmester curve) in a finite region. Taking a point $A_0(x_0, y_0)$ on the dot curve, and selecting the corresponding center point $A_{c1}(x_{c1}, y_{c1})$ on the center point curve, plus the first point $P_1(x_1, y_1)$ of the given three accurate pose points, an 2R open chain rod group can be synthesized. Therefore, all 2R open chain rod groups that can be synthesized within a limited range can form a mechanism scale solution domain.

$$\begin{cases} l = \sqrt{(x_{c1} - x_1)^2 + (y_{c1} - y_1)^2}, \ \varphi_{11} = \arctan\left(\dfrac{y_{c1} - y_0}{x_{c1} - x_0}\right) \\ \varphi_{21} = \arctan\left(\dfrac{y_{c1} - y_1}{x_{c1} - x_1}\right), \ \psi = 180 - \varphi_{21} - \theta_1 \end{cases} \qquad (12)$$

where, l is the length of rod L_2; φ_{11} is the initial angle of rod L_1; φ_{21} is the initial angle of rod L_2; and ψ is the angle of the mark line.

4 Mechanism parameter optimization and analysis

4.1 Determination of optimization objective

For the variable differential gear train planting mechanism designed in this paper, the key to ensure its working quality is to optimize the trajectory shape and key point posture formed by duckbill shaped planter tip. The planting mechanism catches the bowl seedlings dropped by the seedling pick-up mechanism at the highest point of the trajectory. The seedling mouth of the duckbill shaped planter should be as vertical as possible to the direction of the bowl when the seedling is picked up, and the angle between the duckbill shaped planter and the horizontal direction should be as small as possible during the period from the preparation of the seedling to the end of the seedling; During the planting operation, the duckbill shaped planter was obliquely inserted into the ridge surface from the front of the lowest point of planting, and then gradually deflected to the vertical direction of the ridge surface. At the lowest point of planting, the duckbill shaped planter was basically perpendicular to the ridge surface. The area of the contact area between the duckbill shaped planter and the soil depended on the size of the loop formed by the dynamic trajectory. If the contact area was too large, it might lead to the excessive width of the dynamic hole and affect the uprightness of the pot seedlings.

Based on the above analysis, the melon seed trajectory shown in Figure 4 is proposed. The ABC section is the seedling section, and the B point is the highest point of the trajectory. The CD segment is the seedling moving segment, and the duckbill is planted to hold the seedling movement; the DEF segment is the planting segment, and E is the lowest point of planting; FA is the return section, duckbill shaped planter to prepare for the next seedling, complete a cycle, the arrow is shown as the moving direction of duckbill shaped planter on the trajectory.

In this study, vegetable pot seedlings are used as planting objects, and three planting trajectories with key point position information are interpolated and fitted to 300 mm, 400 mm and 500 mm plant spacing respectively. In order to reduce the damage of pot seedlings by planting mechanism at work and improve the verticality and planting success rate of pot seedlings, the following optimization objectives are proposed :

(1) The angle between the highest point of the trajectory and the horizontal direction should be 85°-105° to improve the success rate of seedling grafting and reduce the damage of pot seedling matrix.

(2) The height of vegetable pot seedlings used in the experiment is generally about 140 mm. In order to realize the smooth seedling of duckbill shaped planter and the overall size is not too large, the length of duckbill shaped planter should be between 180-210 mm.

(3) The angle between the duckbill shaped planter and the ridge surface should be 75°-115° when it enters and leaves the ridge surface, which is conducive to punching holes.

(4) In order to achieve the purpose of "zero speed" planting, reduce the width of the hole and solve the problem that the duckbill shaped planter begins to withdraw from the hole to the height of the pot seedling after the completion of the planting operation. The absolute motion trajectory of the tip of the duckbill shaped planter must form a "ring buckle" of suitable size, the height of the ring buckle is greater than 50 mm, and the width is less than 20 mm.

4.2 Computer aided optimization design software

The variable differential gear train planting mechanism designed in this paper has the characteristics of multivariable, nonlinear and coupling[27,28]. Therefore, according to three-position motion generation method. Based on the GUI module of Matlab software, a visual auxiliary optimization design software for human-computer interaction is developed, which simplifies the calculation process and shortens the development cycle. The software interface is shown in Figure 5, and there are 7 functional modules: Module 1 is the pose point parameter input interface. The parameter input boxes of each pose point are abscissa, ordinate and azimuth from left to right, A_0–A_c is the proposed crank length. The software displays the Burmeister curve in Module 7 (graphical display area) according to the set parameters. Module 2 is the dimension synthesis interface. By limiting the length of the crank, the solution domain of the Burmester curve can be formed. By limiting the length of the swing rod (connecting rod), the solution domain of the mechanism can be preliminarily screened, and the number of mechanisms that meet the conditions is displayed on the current interface. Module 3 is the input interface of control points. The introduction of control points makes the adjustment of trajectory shape more flexible. '1-2' refers to the control points inserted between P_1, P_2, and '2-3' and '3-1' are also available. According to the input control point parameters, the software shows the number of mechanisms and crank steering that meet the conditions after the second screening in the current interface. In module 5 (mechanism parameter display area), the center point, circle point coordinates, crank length, swing rod (connecting rod) length, line angle and initial angle of crank and swing rod (connecting rod) of the current demonstration mechanism are displayed. In module 7 (graphic display area), the rotation angle diagram, transmission ratio curve, planting static trajectory and rod group demonstration animation are displayed. Module 4 is the section curve generation interface. Module 5 is the mechanism parameter display area. The module 6 is the rod group trajectory generation interface. Module 7 is the graphic display area.

The human-computer interaction interface of the software can quickly calculate the number of solutions in the feasible region according to the pose points and rod length range parameters input each time, and update the basic parameters, transmission ratio curve and simulation trajectory of the custom selected mechanism in the display area. Retain the mechanism that meets the design requirements in the feasible region, select a set of optimal solutions, determine the length of the rod L_1, and solve the basic parameters. Through the software, the absolute motion and relative motion of the rod group are simulated and compared, and the coordinates of the two control points are continuously adjusted to optimize the size of the loop formed by the dynamic trajectory, so that it can meet the proposed optimization goals and related agronomic requirements.

4.3 Mechanism design and parameter optimization results

The computer-aided optimization design software is used to design the variable differential gear train planting mechanism. Firstly, according to the pose requirements of the seedling point, the seedling point and the planting point, three accurate pose points and their azimuth angles that constrain the planting trajectory are determined. The specific parameters are listed in Table 1. The value range of the abscissa of the center point is set to be 0-300 mm, the value range of the crank length is 130-140 mm, the value range of the connecting rod length is 190-200 mm, and the solution step size is 1 mm.
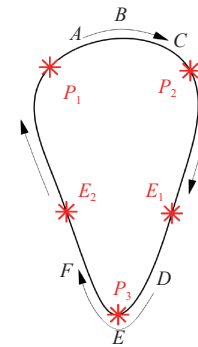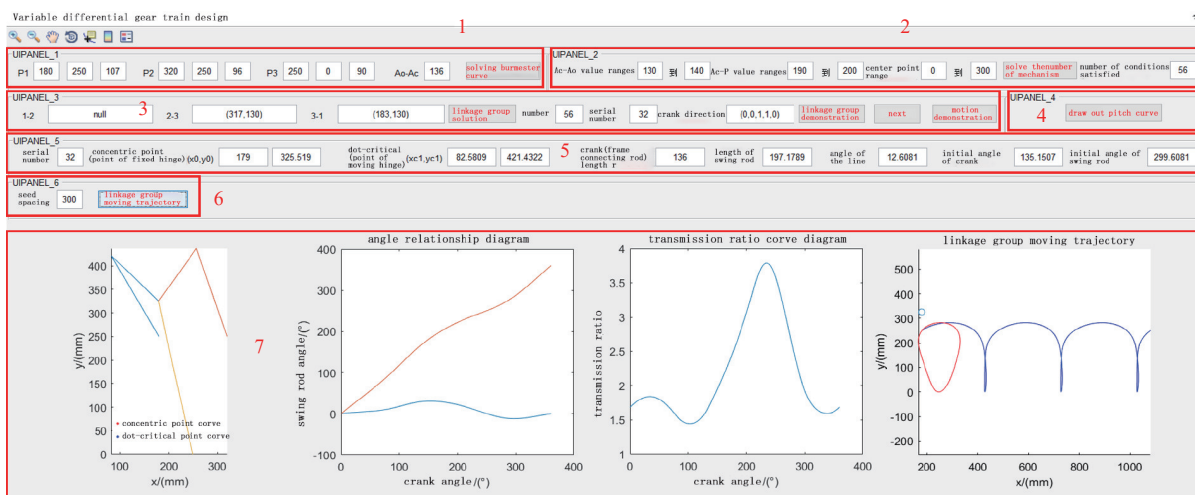
Figure 4   Melon seed type trajectory

Figure 5   Software interface

Table 1   Three precise pose point parameters

P_i	x_i/mm	y_i/mm	θ_i/(°)
1	180	250	107
2	320	250	96
3	250	0	90

After quickly calculating the number of solutions in the feasible region, the simulation trajectory of each mechanism can be drawn. In the design process, it is found that the selection of control points has a significant influence on the trajectory shape. As shown in Figure 4, the control points E_1 and E_2 are arranged on both sides of the original trajectory waist. As the horizontal distance between the

two control points increases, the static trajectory curve near the planting point P_3 will gradually widen.

Taking the plant spacing of 300 mm as an example, the coordinates of the two control points are adjusted, as shown in Figure 6a. If the horizontal distance between the two control points is too small, the waist of the static trajectory curve becomes narrower, and the dynamic trajectory cannot form a buckle. As

shown in Figure 6b, if the horizontal distance between the two control points is too large, the waist of the static trajectory curve becomes wider, the buckle formed by the dynamic trajectory is too large, the hole width formed on the soil surface will be too large, the pot seedlings are prone to lodging, and the uprightness of seedlings is affected. The better dynamic trajectory curve is shown in Figure 6c.

a. No buckle   b. Too large buckle   c. Optimal buckle
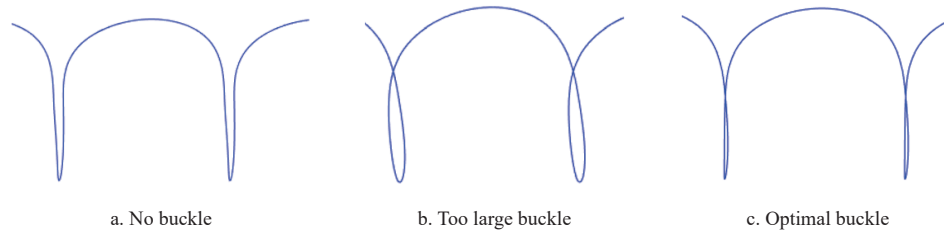
Figure 6   Trajectory shape and control point position

After several debugging and optimization, the coordinates of the two control points are determined to be (317,130) and (183,130) respectively. The basic parameters of the optimal solution of the mechanism are listed in Table 2.

Based on the preferred mechanism parameters, the coordinates of the two control points adapted to the 400 mm plant spacing were determined to be (330,130) and (170,130), and the coordinates of the two control points adapted to the 500 mm plant spacing were determined to be (350,130) and (150,130).

Using the three-order non-uniform B-spline interpolation fitting algorithm[29,30], three planting trajectories with key point position information adapted to 300 mm, 400 mm and 500 mm plant spacing are obtained, and the total transmission ratio of three groups of variable differential gear trains is inversely solved. Under the

condition that the transmission ratio of the positive gear pair and the transmission ratio of the differential gear train are known, the sub-transmission ratio of the single-stage non-circular gear pair is calculated and the pitch curves of three pairs of non-circular gears are solved. The calculation results are shown in Figure 7.

Table 2   Basic parameters of optimal mechanism

Parameters	Value
A_0/mm	(179, 325.5)
A_c/mm	(82.6, 421.4)
r/mm	136
l/mm	197
φ_{11}/(°)	135.2
φ_{21}/(°)	299.6

a. 300 mm spacing   b. 400 mm plant spacing   c. 500 mm plant spacing
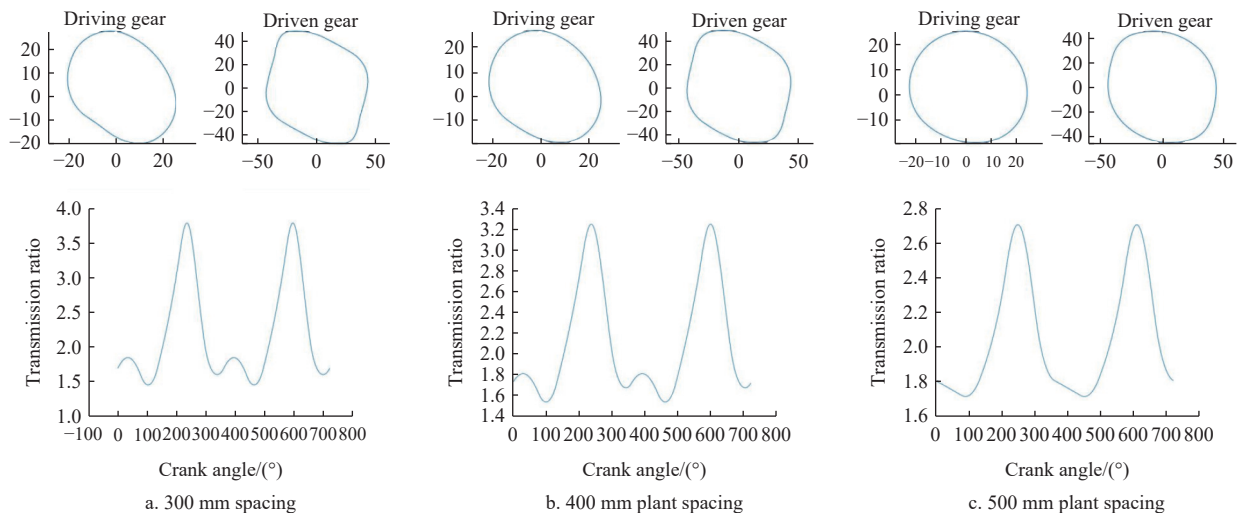
Figure 7   Noncircular gear pitch curve and transmission ratio

5 Virtual prototype simulation and physical prototype test

5.1 Virtual prototype simulation

Based on the optimized mechanism parameters, the overall structure design of the variable differential gear planting mechanism is carried out. The three-dimensional modeling of three sets of planting mechanisms is completed by Solidworks. Imported this modeling into ADAMS software, and the constraints are added for

motion simulation. As shown in Figure 8, the simulation results of static trajectory and dynamic trajectory are compared with the results in computer aided optimization design software.

The marking measurement method in ADAMS software was employed to verify that the three sets of theoretical trajectories and simulated trajectories in Figure 8 are essentially identical. This further confirms the correctness and feasibility of the three-dimensional structure design of the planting mechanism.
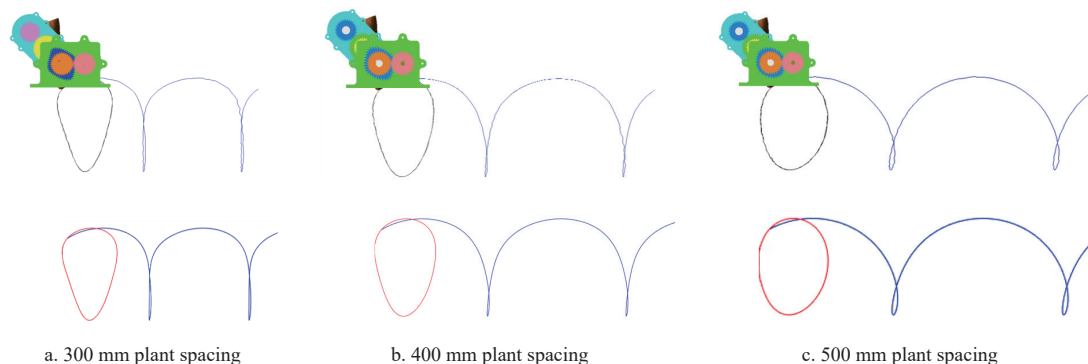
a. 300 mm plant spacing   b. 400 mm plant spacing   c. 500 mm plant spacing

Figure 8   Trajectory comparison

5.2   Physical prototype construction and idling test

In order to further explore the actual working conditions of the planting mechanism[31,32], a variable differential gear train planting mechanism test bench was built. Most of the parts of the mechanism used 3D printed parts. During the test, the manual seedling throwing method was used to match the speed of the conveyor belt and simulate the field working state of the mechanism. The planting mechanism rotates around fixed hinge, and the soil trough moves linearly relative to the mechanism. The test bench is shown in Figure 9.
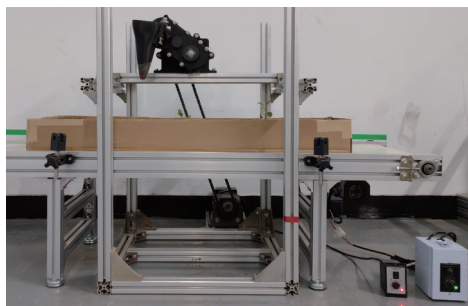

Figure 9   Planting mechanism test bench

Starting from the initial position of the crank and connecting rod, the idling test of the physical prototype was carried out. As shown in Figure 10, taking 300 mm plant spacing as an example, the actual posture and theoretical posture of the duckbill shaped planter at each key point (seedling point, seedling point, planting point) were verified by high-speed camera. After actual measurement, the seedling point of each three trajectories was the highest point of the trajectory, and the angle between the duckbill shaped planter and the horizontal direction at this point was 96°, which met the first optimization goal. The length of the connecting rod is 197 mm, which meets the second optimization goal. The angles between the duckbill shaped planter and the ridge surface were 77.82°, 80.44° and 86.02° respectively when it entered the ridge surface under different plant spacing conditions, and the angles between the duckbill shaped planter and the ridge surface were 112.82°, 109.86° and 104.54° respectively when it left the ridge surface, which met the third optimization goal. The heights of each trajectory of the end of planter under different plant spacing conditions are 140 mm, 60 mm and 86 mm, and the widths are 8 mm, 9 mm and 12 mm, which meets the fourth optimization goal.
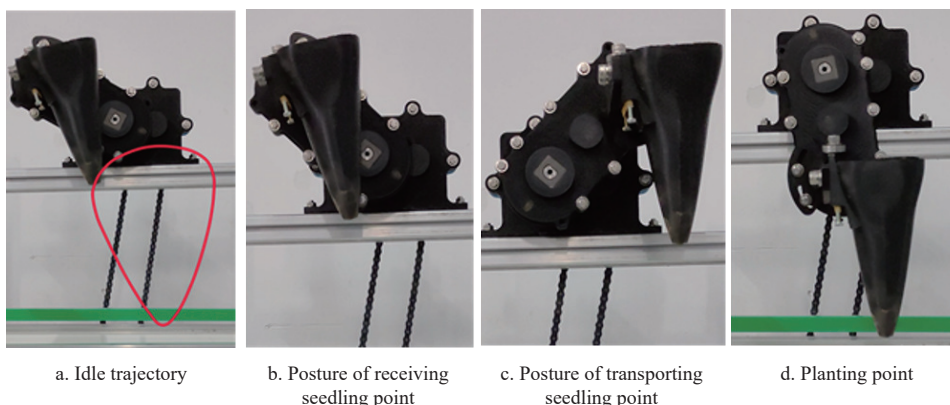

a. Idle trajectory   b. Posture of receiving seedling point   c. Posture of transporting seedling point   d. Planting point

Figure 10   Results of idling test

5.3   Planting tests

Because three planting trajectories adapted to different plant spacing were fitted, three planting experiments were carried out, and 100 pot seedlings were planted in each experiment. The transformation of planting trajectory was realized by replacing the single-stage non-circular gear pair in the fixed-axis gear train. The standard quantification of the planting effect is defined as: when the angle between the planted pot seedling and the horizontal plane is greater than 70°, the pot seedling has a good uprightness and is identified as successful planting. The planting effects are shown in

Figure 11, and the test results are listed in Table 3. At the same time, the planting success rate, the actual average plant spacing and the widths of the moving hole are counted. The widths of the moving hole should be between 60-80 mm.

The test dates show that plant spacing errors are within ±5 mm, and the planted pot seedlings have good uprightness, high success rates, and suitable widths of the moving hole, indicating that the variable differential gear train planting mechanism can adapt to a variety of plant spacing.
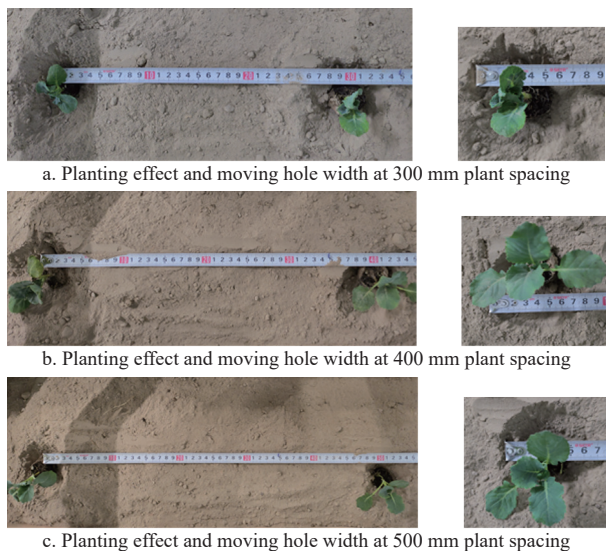
a. Planting effect and moving hole width at 300 mm plant spacing

b. Planting effect and moving hole width at 400 mm plant spacing

c. Planting effect and moving hole width at 500 mm plant spacing

Figure 11   Planting effect

Table 3   Experiment results of 3 plant spacing planting

Theoretical plant spacing/mm	Test sample size/plant	Planting success rate/%	Actual average plant spacing/mm	Spacing error/%	width of the moving hole/mm
300	100	94	303	1.3	72
400	100	96	402	1.25	70
500	100	95	503	1.88	71

6   Conclusions

(1) A variable differential gear train planting mechanism based on precise poses and trajectory controls was proposed. The overall structure, transmission mode and working principle of the mechanism were analyzed.

(2) According to the pose requirements of receiving seedling point, transporting seedling point and planting point, three precise pose points of constrained planting trajectory were determined. Through the three-position motion generation structural synthesis method, combined with the visual computer-aided optimization design software of human-computer interaction, a set of mechanism parameters that meet the planting requirements were selected: A_0(179, 325.5), A_c(82.6, 421.4), r=136 mm, l=197 mm, φ_{11}=135.2º, φ_{21}=299.6º. Based on the optimized mechanism parameters, by only changing the coordinates of two trajectory shape control points, three planting trajectories with key point position information suitable for 300 mm, 400 mm and 500 mm plant spacing were obtained by using the cubic non-uniform B-spline interpolation fitting algorithm, and the total transmission ratio of three groups of variable differential gear trains were calculated and distributed.

(3) Three pairs of single-stage non-circular gear pairs with different transmission ratios were replaced in turn and three sets of planting mechanisms were modeled in three dimensions, and the virtual prototype motion simulation is completed by ADAMS software. The test results demonstrated the alignment between the theoretical solution and the actual test's attitude and trajectory, thus confirming the accuracy and feasibility of the three-dimensional structure design of the planting mechanism.

(4) The test bench of variable differential gear train planting mechanism was built to simulate the field working state of the mechanism, and the idling test and planting test were carried out. The idling test proved that the physical prototype met the four optimization objectives. The planting test showed that when the

sample size was 100 pot seedlings, the actual average plant spacing were 303 mm, 402 mm, 503 mm, the errors were 1.3 %, 1.25 %, 1.88 %, the widths of the moving hole were 72 mm, 70 mm, 71 mm, and the planting success rates were 94 %, 96 %, 95 %. The test results confirmed the accuracy of the mechanism optimization design, indicating that the variable differential gear train planting mechanism is versatile, capable of accommodating different plant spacings, and exhibits effective planting outcomes.

[References]

[1] Xin Z L, Cui Y J, Yang X W, Kong L B, Lin Q. Current situation of global vegetable industry and research progress of vegetable breeding development path in China. Molecular Plant Breeding, 2022; 20(9): 3122–3132. (in Chinese)

[2] Bai J Q, Hao F Q, Cheng G H, Li C G. Machine vision-based supplemental seeding device for plug seedling of sweet corn. Computers and Electronics in Agriculture, 2021; 188: 106345.

[3] Shao Y Y, Liu Y, Xuan G T, Hu Z C, Han X, Wang Y X, et al. Design and test of multifunctional vegetable transplanting machine. IFAC-PapersOnLine, 2019; 52(30): 92–97.

[4] Wen Y S, Zhang J X, Tian J Y, Duan D S, Zhang Y, Tan Y Z, et al. Design of a traction double-row fully automatic transplanter for vegetable plug seedlings. Computers and Electronics in Agriculture, 2021; 182: 106017.

[5] Sun L, Zheng G H, Ye Z Z, Yu G H. Structural synthesis and innovative design of multi-link planting mechanism based on graph theory. Transactions of the CSAM, 2022; 53(5): 67–74. (in Chinese)

[6] Han C J, Hu X W, Zhang J, You J, Li H L. Design and testing of the mechanical picking function of a high-speed seedling auto-transplanter. Artificial Intelligence in Agriculture, 2021; 5: 64–71.

[7] Han L H, Mao H P, Zhao H M, Liu Y, Hu J P, Ma G X. Design of root lump loosening mechanism using air jets to eject vegetable plug seedlings. Transactions of the CSAE, 2019; 35(4): 37–45. (in Chinese)

[8] Yang Q Z, Huang G L, Shi X Y, He M S, Ahmad I, Zhao X Q, et al. Design of a control system for a mini-automatic transplanting machine of plug seedling. Computers and Electronics in Agriculture, 2020; 169: 105226.

[9] Ye B L, Yi W M, Yu G H, Gao Y, Zhao X. Optimization design and test of rice plug seedling transplanting mechanism of planetary gear train with incomplete eccentric circular gear and non-circular gears. Int J Agric & Biol Eng, 2017; 10(6): 43–55.

[10] Khadatkar A, Mathur S M, Dubey K, Bhusanababu V. Development of embedded automatic transplanting system in seedling transplanters for precision agriculture. Artificial Intelligence in Agriculture, 2021; 5: 175–184.

[11] Zhao X, Guo J L, Li K W, Dai L, Chen J N. Optimal design and experiment of 2-DoF five-bar mechanism for flower seedling transplanting. Computers and Electronics in Agriculture, 2020; 178: 105746.

[12] Paradkar V, Raheman H, K R. Development of a metering mechanism with serial robotic arm for handling paper pot seedlings in a vegetable transplanter. Artificial Intelligence in Agriculture, 2021; 5: 52–63.

[13] Mazzetto F, Calcante A. Highly automated vine cutting transplanter based on DGNSS-RTK technology integrated with hydraulic devices. Computers and Electronics in Agriculture, 2011; 79(1): 20–29.

[14] Yu G H, Wang L, Sun L, Zhao X, Ye B L. Advancement of mechanized transplanting technology and equipments for field crops. Transactions of the CSAM, 2022; 53(9): 1–20. (in Chinese)

[15] Li P B, Yan H, Wang P L, Wu H H, Han L H. Optimization and test of

small plant spacing planting mechanism rod for transplanter. Transactions of the CSAM, 2020; 51(S2): 72–78. (in Chinese)

[16] Zhao X, Liao H W, Ma X X, Dai L, Yu G H, Chen J N. Design and experiment of double planet carrier planetary gear flower transplanting mechanism. Int J Agric & Biol Eng, 2021; 14(2): 55–61.

[17] Chen J N, Zhang P H, Wang Y, Xia X D, Jiang C Q. Multi-objective parameter optimization and experiment of rotary seedling planting mechanism. Transactions of the CSAM, 2015; 46(05): 46–53. (in Chinese)

[18] Chen J N, Huang Q Z, Wang Y, Sun L, Zhao X, Wu C Y. Parametric analysis and inversion of transplanting mechanism with planetary non-circular gears for potted-seedling transplanter. Transactions of the CSAE, 2013; 29(8): 18–26. (in Chinese)

[19] Ye B L, Zeng G J, Deng B, Yang C L, Liu J K, Yu G H. Design and tests of a rotary plug seedling pick-up mechanism for vegetable automatic transplanter. Int J Agric & Biol Eng, 2020; 13(3): 70–78.

[20] Gouda E, Mezani S, Baghli L, Rezzoug A. Comparative study between mechanical and magnetic planetary gears. IEEE Transactions on Magnetics, 2011; 47(2): 439–450

[21] Yang T, Han J, Yin L R. A unified synthesis method based on solution regions for four finitely separated and mixed "Point-Order" positions. Mechanism and Machine Theory, 2011; 46(11): 1719–1731.

[22] Lin S, Liu J, Wang H, Zhang Y. A novel geometric approach for planar motion generation based on similarity transformation of pole maps. Mechanism and Machine Theory, 2018; 122: 97–112.

[23] Jin X, Li D Y, Ma H, Ji J T, Zhao K X, Pang J. Development of single row automatic transplanting device for potted vegetable seedlings. Int J Agric & Biol Eng, 2018; 11(3): 67–75.

[24] Antonov A, Glazunov V. Position, velocity, and workspace analysis of a novel 6-DOF parallel manipulator with "piercing" rods. Mechanism and Machine Theory, 2021; 161: 104300.

[25] Sun L, Xong Z Q, Xu Y D, Liu B, Yu G H, Wu C Y. Transplanting mechanism of rice seedling based on precise multi-position analysis. Transactions of the CSAM, 2019; 50(9): 78–86. (in Chinese)

[26] Wang L, Sun L, Huang H M, Yu Y X, Yu G H. Design of clamping-pot-type planetary gear train transplanting mechanism for rice wide–narrow-row planting. Int J Agric & Biol Eng, 2021; 14(2): 62–71.

[27] Sun L, Chen X, Wu C Y, Zhang G F, Xu Y D. Synthesis and design of rice pot seedling transplanting mechanism based on labeled graph theory. Computers and Electronics in Agriculture, 2017; 143: 249–261.

[28] Yu G H, Liao Z P, Xu L H, Zhao P, Wu C Y. Optimization design and test of large spacing planetary gear train for vegetable pot-seedling planting mechanism. Transactions of the CSAM, 2015; 46(7): 38–44. (in Chinese)

[29] Suruchi S, Swarn S, Anu A. Cubic B-spline method for non-linear sine-Gordon equation. Computational and Applied Mathematics, 2022; 41(8): 382.

[30] Riboli M, Corradini F, Silvestri M, Aimi A. A new framework for joint trajectory planning based on time-parameterized B-splines. Computer-Aided Design, 2023; 154: 103421.

[31] Xu C L, Lu Z J, Xin L, Wng J, Zhao Y. Optimization design and experiment of walk-type potted rice seedling transplanting mechanism on film perforating part. Transactions of the CSAM, 2019; 50(8): 90–96. (in Chinese)

[32] Xu C L, Lu Z J, Xin L, Zhao Y. Optimization design and experiment of full-automatic strawberry potted seedling transplanting mechanism. Transactions of the CSAM, 2019; 50(8): 97–106. (in Chinese)